

## Analysis of hydrochemical characteristics and genesis of water-deficient rivers in China: a case study of the Ciyao River Basin in Shanxi Province

Hui Xiao-Mei, Yuan Jin\*, Li Chao, Fan Xiao-Jun, Zhou Yuan

College of Environmental Science and Engineering, Taiyuan University of Technology, Jinzhong, China

**\*Corresponding Author:** Yuan Jin, College of Environmental Science and Engineering, Taiyuan University of Technology, Jinzhong 030600, China. Email: [yuanjin@tyut.edu.cn](mailto:yuanjin@tyut.edu.cn)

Received: 10 October 2022; Accepted: 20 November 2022; Published: 1 January 2023

© 2023 Codon Publications

OPEN ACCESS



RESEARCH ARTICLE

### Abstract

In order to explore the chemical water characteristics of water-scarce rivers in China, the Ciyao River basin in Shanxi Province was taken as a case study. Water samples of the mainstream and its tributaries were collected in the wet, normal, and dry seasons of 2021. The composition and spatial variation of the main ions in the water body were analyzed using the ion chromatography (IC) instrument. In addition, Pearson correlation analyses were used to evaluate relevant correlation between ion concentrations. The results showed that the overall surface water in the study area was weakly alkaline, and the content of total dissolved solids (TDS) varied greatly, ranging from 702 to 5091 mg/L, with an average of 2897 mg/L. The TDS showed a middle stream > downstream > upstream trend, and the hydrochemical type was  $\text{Cl} \cdot \text{SO}_4 \cdot \text{HCO}_3 - \text{Ca} \cdot \text{Na}$ . The contents of most ions were significantly changed based on differences in sampling sites and seasons. Natural and human factors influence the chemical characteristics of the river. According to the Gibbs diagram and Piper diagram (Figure 3), the ionic composition of the water body in the basin is mainly affected by the joint action of rock weathering and evaporative crystallization. Carbonate rocks constitute the most significant rock weathering, followed by evaporative and silicate rocks. Wastewater from industrial enterprises, agricultural wastewater, and activities of people's daily living also have some influence on rock weathering. Cation exchange is also important in forming chemical water components in the Ciyao River. The research results can provide technical references and a basis for regional water environment protection, water resources development and utilization, and watershed eco-hydrology research.

**Keywords:** Ciyao River Basin; evaporation crystallization; hydrochemical characteristics; ion sources; rock weathering

### Introduction

Environmental chemical pollution has caused many health concerns in the last two decades (Ge *et al.*, 2019; Ke *et al.*, 2022; Lin *et al.*, 2021; Liu *et al.*, 2022; Peng *et al.*, 2021; Tian *et al.*, 2021; Wu *et al.*, 2021; Yang *et al.*, 2021; Yin *et al.*, 2021, 2022; Zhang *et al.*, 2019, 2022; Zhao *et al.*, 2021). The chemical composition of water is the result of long-term interaction between the water body and the

surrounding environment in the process of circulation (Bai *et al.*, 2022; Chen *et al.*, 2021; Dai *et al.*, 2022; Fang *et al.*, 2021; Liu *et al.*, 2020; Quan *et al.*, 2021; Xu *et al.*, 2021; Zhang *et al.*, 2021). The history of formation and chemical characteristics of water from streams can be indicated in the basin (Pant *et al.*, 2018; Zongxing *et al.*, 2016). Research on the chemical characteristics of water from the water body in the basin can provide important information for understanding the composition

of the basin and its correlation with the environment. Due to the natural conditions such as topography, geology, and climate, and the influences of anthropogenic production and life, changes in water quality will have a range of ecological effects on aquatic ecosystems and largely reflect the characteristics of variations in the basin (Fu *et al.*, 2009). As the Ciyao river flows fast, the alternating period is only 16 days, and the river water that touches the sand and gravel in the riverbed is less, restricting its mineralization. As a result, the hydrochemical properties of river water almost completely rely on the nature and proportion of water sources used for recharge (Ruxue, 2021). Therefore, an understanding of the hydrochemical characteristics and genesis of the basin can greatly contribute to water environment protection programs.

In recent years, some research was conducted on hydrochemical characteristics. It achieved fruitful results, classifying the causes of the presence of hydrochemicals into natural causes and man-made causes. The research focuses mostly on the source of large rivers or areas rich in groundwater resources. For example, the analysis of rivers, lakes, and groundwater focused on the river source region (Wu *et al.*, 2015) of the Yangtze River Basin (Liu *et al.*, 2021a), the Three Gorges Reservoir region (Li *et al.*, 2012), the upper reaches of the Brahmaputra River (Yan *et al.*, 2022), the Basomtso lake (Luo *et al.*, 2021) in Tibet, the Jialing River (Li *et al.*, 2018), the Qin River (Liu *et al.*, 2018), the Hutuo River (Huiwei *et al.*, 2021) and other rivers, lakes, and groundwater sources. The research methods also tend to be diversified (Shen, 1983), including the use of Piper diagram (Li *et al.*, 2022), Gibbs figure (Qi *et al.*, 2021), water quality simulation methods (Jia *et al.*, 2017), and isotope analysis methods (Liu *et al.*, 2019a) through which the chemical characteristics and genesis of river ions were explored.

Compared with other river basins in China, the water chemistry characteristics of water-scarce rivers in the north have not been systematically and deeply studied, and the study of the whole basin and seasonal changes needs to be improved (Zhang *et al.*, 2015a). Therefore, it is necessary to continue to carry out an in-depth study of the water chemistry characteristics of rivers with low natural runoff in the north, mainly relying on the tailwater of sewage plants, to provide a basis for exploring the future exploration of rivers artificially recharged with tailwater and global climate and environmental changes. This paper is based on river water sampling in the main tributaries in the Ciyao River Basin in Shanxi Province in the months of April, June, August, and October 2021, which cover three hydrological periods of wet, normal, and dry seasons, and in combination with the existing environmental background data of the basin, we analyzed the contents and temporal-spatial distribution

characteristics of main cations and anions in water body samples from different sampling segments. We explored the main controlling factors of hydrochemistry to provide basic data for further research on water quality changes in the Ciyao River and a scientific basis for understanding the watershed water environment and resources.

## Material and Method

### Overview of the study area and sample collection and analysis

#### Overview of the study area

The Ciyao River is a primary tributary of the Fenhe River, the second largest tributary of the Yellow River, with a total length of 86.4 km and a total drainage area of 1059.83 km<sup>2</sup>. Originating from the Taling Village in the mountainous area of Jiaocheng County and the Yangtian Pool in the mountainous area of Qingxu County, it is in the central part of Shanxi Province, on the left bank of the middle reach of the Fenhe River, and in the east of the Wenyu River, mainly flowing across three counties (municipalities), namely, Qingxu, Jiaocheng, and Fenyang. West Shihou Village, Jiaocheng, is where the Ciyao River begins and the confluence of the Hupingshi River, the Wayao River, the Dongshihou, and the total escape outlet of sub-channels 1 and 2 of the Fenhe River irrigation area, with a five-finger shaped layout. The range of the watershed is shown in Figure 1.

#### Sample collection and analysis

In accordance with the relevant contents of *Water quality-Guidance on Sampling Techniques* (HJ 494-2009) and the geomorphic characteristics of the Ciyao River Basin, and by taking into account the location of the confluence of various tributaries, seven sampling sites were set up in the trunk stream and tributaries of the Ciyao River: (1) Lingdi; (2) Jiaocheng; (3) Dongshihou; (4) Wuliang, (5) Nanxian; (6) Peihui; and (7) Sangliushu. Sections 1 and 2 are located in the upper reach, sections 3, 4, and 5 are in the middle reach, and sections 6 and 7 are located in the lower reach, and sampling was done in the wet (June and August), normal (April), and dry (October) seasons in 2021.

To maintain the consistency of sampling conditions, we chose the days in which there was no rain for 72 h (Markich and Brown, 1998). Before collecting samples, each sample vial was scrubbed with hydrogen nitrate and then flushed with distilled water. Water samples were collected in 2 L polypropylene vials and passed through a 0.45-mm CA (Cellulose Acetate) membrane filter. The samples were placed in a clean and self-sealing

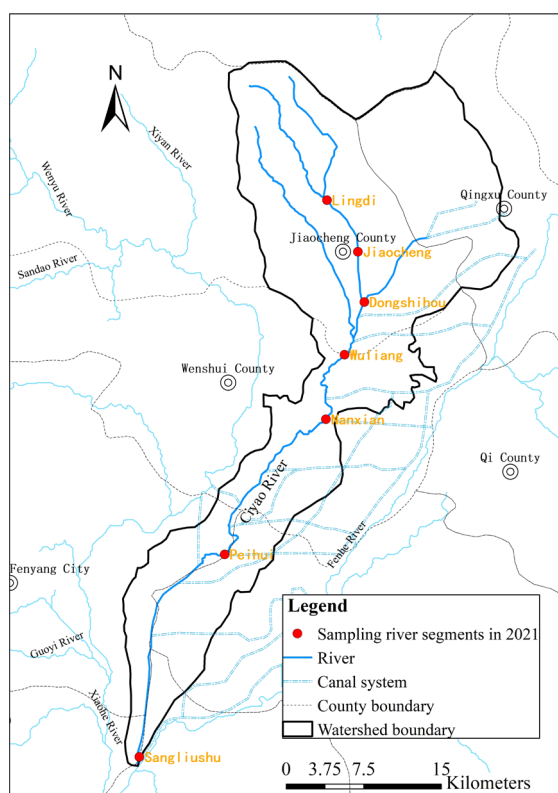


**Figure 1. Catchment plan of Ciyao River.**

polyethylene (PE) bag and stored in the refrigerator at 4°C until a test was conducted.

We collected 21 samples from 7 sites and determined and analyzed 12 key metrics:  $\text{Na}^+$ ,  $\text{K}^+$ ,  $\text{Ca}^{2+}$ ,  $\text{Mg}^{2+}$ ,  $\text{Cl}^-$ ,  $\text{SO}_4^{2-}$ ,  $\text{HCO}_3^-$ ,  $\text{CO}_3^{2-}$ ,  $\text{NO}_3^-$ , total dissolved solids (TDS), total hardness (TH), and pH value. TDS was determined using the dry weight method, TH was determined through complexometric titrations, pH value was determined with an FE-20pH meter (METTLER TOLEDO), and the concentrations of the remaining ions were determined using the ion chromatography (IC) instrument (Thermo Fisher Scientific (China) Co., Ltd.).

### Data analysis

We used spss18.0 to perform statistics and correlation analyses of the contents of hydrochemical ions in various river segments; used Pearson correlation analyses to evaluate relevant relationships in ion concentrations; used Origin 2018 to draw the Piper diagram and the Na end-member diagram for analyzing the influence of hydrochemical types and three major lithological rock types (silicate, carbonate, and evaporite rocks) on solutes in water; and used the Gibbs diagram for qualitatively analyzing main factors controlling the source of solutes in water. Statistical significance was  $P$  value  $< 0.05$ .

## Results and Discussion

### Analysis of major ions

#### Analysis of physical and chemical properties

The surface water in the Ciyao River Basin was weakly alkaline, with a pH value ranging from 7.84 to 8.64 and a mean value of 8.2. Among seven sampling sections, the sampling site in the Nanxian had water bodies with relatively high pH values in its proximity because this place received a large amount of water receding from the farmland and wastewater from the farms nearby. From Table 1, it can be seen that the water body is more weakly alkaline in June than in other months because June belongs to the wet season in which it rains a lot; TDS ranged from 324 mg/L to 7947 mg/L with the mean value of 2257 mg/L and holistically TDS in the middle reach was greater than that in the lower reach. TDS in the lower reach was greater than in the upper reach because the area in the middle reach is densely populated with many industries that often discharged wastewater to the river, leading to an increase in TDS. In contrast, the area on the upper reach is dominated by forest land and bushes, with vegetation having strong abilities to constrain sediments, resulting in reduced TDS. The area on the lower reach is an agricultural land-dominated area, where serious soil and water loss occurred, and TDS responses increased (Williams *et al.*, 1997); TH ranged from 44 mg/L to 1844 mg/L, with the mean value of 396.49 mg/L. The hardness of the water body in the Ciyao River Basin is on the higher side. According to the classification of the hardness of water, the water in the Lingdi and the Nanxian is soft, Dongshihou is very hard water, and the water in other sampling sites is the hardest. There are some differences in the physical and chemical properties of water bodies from different river segments in the Ciyao River Basin due to topography, geomorphy, and local climate (DeVivo *et al.*, 2017).

#### Contents of major ions in rivers

The chemical composition of natural water is the result of many direct and indirect factors (Li *et al.*, 2002). Direct factors include the chemical composition and properties of rocks and soil, the vital activities of organisms, and human activities (Liu *et al.*, 2021b); indirect factors refer to conditions that decide the interactions between substances and water. According to the component characteristics (Table 1) of major ions in the Ciyao River in different months, the ranges of the equivalent concentrations of cations  $\text{Na}^+$ ,  $\text{K}^+$ ,  $\text{Ca}^{2+}$ , and  $\text{Mg}^{2+}$  in surface water in the Ciyao River in 2021 were 12.20–559.00 mg/L (with the mean value of 225.90 mg/L), 2.49–340.00 mg/L (55.75 mg/L), 34.40–1650.00 mg/L (342.67 mg/L), and 9.88–194.00 mg/L (60.42 mg/L), respectively, and the

Table 1. Analysis results of main ion components in Ciyao River surface water (mg/L).

Month	Item	pH	TDS	TH	Na <sup>+</sup>	K <sup>+</sup>	Ca <sup>2+</sup>	Mg <sup>2+</sup>	Cl <sup>-</sup>	SO <sub>4</sub> <sup>2-</sup>	HCO <sub>3</sub> <sup>-</sup>	CO <sub>3</sub> <sup>2-</sup>	NO <sub>3</sub> <sup>-</sup>
4 April	Max.	7.91	324.00	44	12.20	3.48	34.40	9.88	25.80	46.90	160.00	5.74	6.20
	Min.	8.49	7190.00	1316	363.00	157.00	1180.00	136.00	3130.00	1390.00	464.00	48.80	166.00
	Mean	8.10	2560.86	389.27	194.31	58.34	344.07	45.20	800.51	495.70	224.43	19.22	59.33
	Standard deviation	0.2028	2264.39	436.64	121.51	52.94	393.67	43.37	1076.68	437.99	108.94	13.76	52.61
	Coefficient of variation	0.025	0.88	1.12	0.63	0.91	1.14	0.96	1.34	0.88	0.49	0.72	0.89
6 June	Max.	7.44	1096.00	87.90	136.00	4.03	62.10	22.60	180.00	199.00	86.00	5.00	17.94
	Min.	8.72	7947.00	1844.00	300.00	340.00	1650.00	194.00	2650.00	645.00	288.00	28.00	465.15
	Mean	7.98	3070.57	608.96	238.14	100.58	530.73	78.23	980.29	396.14	209.14	8.29	119.33
	Standard deviation	0.436	2556.82	639.11	73.64	116.04	574.15	65.69	945.72	160.84	82.22	8.69	159.84
	Coefficient of variation	0.055	0.83	1.05	0.31	1.15	1.08	0.84	0.96	0.41	0.39	1.05	1.34
8 August	Max.	8.20	811.00	133.50	124.00	4.83	114.00	19.50	43.30	91.00	94.90	0.00	14.13
	Min.	8.71	2800.00	445.30	559.00	43.80	362.00	88.30	601.00	219.00	269.00	34.00	128.47
	Mean	8.51	1846.57	267.41	288.17	28.22	215.50	60.13	339.38	150.33	187.82	5.67	73.90
	Standard deviation	0.1779	783.51	107.35	171.10	13.32	90.77	28.68	210.80	52.20	71.56	13.88	43.10
	Coefficient of variation	0.021	0.42	0.401	0.59	0.47	0.42	0.48	0.62	0.35	0.38	2.45	0.58
10 October	Max.	7.52	580.00	145.4	58.50	2.49	121.00	19.40	26.20	224.00	215.00	0.00	19.09
	Min.	8.43	2430.00	654.9	409.00	63.40	571.50	113.00	495.00	943.00	489.00	0.00	91.70
	Mean	7.98	1550.14	320.31	191.87	31.93	262.21	58.09	313.81	479.21	264.50	0.00	64.43
	Standard deviation	0.86	696.60	177.79	118.21	21.06	156.02	34.81	184.16	268.24	99.27	0.00	26.92
	Coefficient of variation	0.11	0.45	0.56	0.62	0.66	0.60	0.60	0.59	0.56	0.38	—	0.42
The whole year	Max.	7.44	324.00	44	12.20	2.49	34.40	9.88	25.80	46.90	86.00	0.00	6.20
	Min.	8.74	7947.00	1844	559.00	340.00	1650.00	194.00	3130.00	1390.00	489.00	48.80	465.15
	Mean	8.09	2257.04	396.49	225.90	55.75	342.67	60.42	618.47	388.87	222.72	8.39	79.44
	Standard deviation	0.92	1790.30	400.33	122.59	69.00	366.11	44.91	759.88	292.89	91.43	12.27	87.54
	Coefficient of variation	0.11	0.79	1.01	0.54	1.24	1.07	0.74	1.23	0.75	0.41	1.46	1.10

TDS, total dissolved solids; TH, total hardness.

ranges of the equivalent concentrations of anions  $\text{Cl}^-$ ,  $\text{SO}_4^{2-}$ ,  $\text{HCO}_3^-$ ,  $\text{CO}_3^{2-}$ , and  $\text{NO}_3^-$  in surface water in the Ciyao River in the same year were 25.80–3130.00 mg/L (618.47 mg/L), 46.90–1390.00 mg/L (388.87 mg/L), 86.00–489.00 mg/L (222.72 mg/L), 0.00–48.80 mg/L (8.39 mg/L), and 6.20–465.15 mg/L (79.44 mg/L), respectively. The order of the main cations by the average content from high to low is  $\text{Ca}^{2+} > \text{Na}^+ > \text{Mg}^{2+} > \text{K}^+$ .  $\text{Ca}^{2+}$  possesses 50% of the total content of the cations, and  $\text{Na}^+$  possesses 33% of the total content of the cations. The order of the main anions by the average annual content from high to low is  $\text{Cl}^- > \text{SO}_4^{2-} > \text{HCO}_3^- > \text{NO}_3^- > \text{CO}_3^{2-}$ .  $\text{Cl}^-$  occupies 46.93% of the total content of the anions, and  $\text{SO}_4^{2-}$  occupies 29.5% of the total content of the anions, whereas  $\text{CO}_3^{2-}$  occupies only 0.6% of the total content of the anions. This indicates that major ions in the Ciyao River Basin were influenced by the dissolution of evaporite rocks and carbonates (Ning *et al.*, 2016).

#### Temporal-spatial distribution characteristics of major ions

The characteristics of contents of ions in different river segments are shown in Figure 2. Cations in surface water in different river segments in the Ciyao River Basin in different months are dominated by  $\text{Ca}^{2+}$  and  $\text{Na}^+$ . The portion of the total number of  $\text{Ca}^{2+}$  and  $\text{Na}^+$  in the total number of cations in April, June, August, and October was 83.87, 81.13, 84.97, and 83.46%, respectively. There is a big difference between the contents of anions in different river segments, with Lingdi dominated by anions  $\text{SO}_4^{2-}$  and  $\text{HCO}_3^-$ ; Jiaocheng by  $\text{Cl}^-$  and  $\text{SO}_4^{2-}$  in April, and  $\text{SO}_4^{2-}$  and  $\text{HCO}_3^-$  in June, August, and October;

Dongshihou by  $\text{Cl}^-$  and  $\text{SO}_4^{2-}$ ; Wuliang section by  $\text{HCO}_3^-$  in April,  $\text{Cl}^-$  in June and August,  $\text{Cl}^-$ ,  $\text{SO}_4^{2-}$ , and  $\text{HCO}_3^-$  in October; the mouth, through which Nanxian by  $\text{Cl}^-$  and  $\text{HCO}_3^-$ ; Peihui and Sangliushu by  $\text{Cl}^-$  and  $\text{SO}_4^{2-}$ .

The coefficient of variation (CV) is a statistic that measures the degree of variations in various observed values. Normally, a CV of 0–0.15 indicates a relatively low variation, a CV of 0.16–0.35 indicates a moderate variation, and a CV larger than 0.36 indicates a high variation. The values of the coefficients of variation of major ions in surface water in the Ciyao River show that the contents of various ions fluctuated wildly.

The concentrations of ions vary greatly from one sampling site to another. Viewing from the spatial distribution,  $\text{Cl}^-$ ,  $\text{SO}_4^{2-}$ , and  $\text{NO}_3^-$  holistically show a trend of middle reach > lower reach > upper reach. Forest and bush lands are dominant in the upper beach of the river, and agricultural and construction lands are dominant in the middle and downstream. Differences in the type of land use have some influences on hydrochemical characteristics. The areas of upper reaches are forest land and bush areas where there are very few human activities and basically no industrial enterprises, so the share of various anions is also small. The Jiaocheng, Dongshihou, Nanxian, and Wuliang section in the middle reach are construction land-dominated areas with a dense population. Especially, on the banks of the Dongshihou, there are many enterprises. In the Wuliang section in Wenshui county, there are a lot of houses that discharge domestic

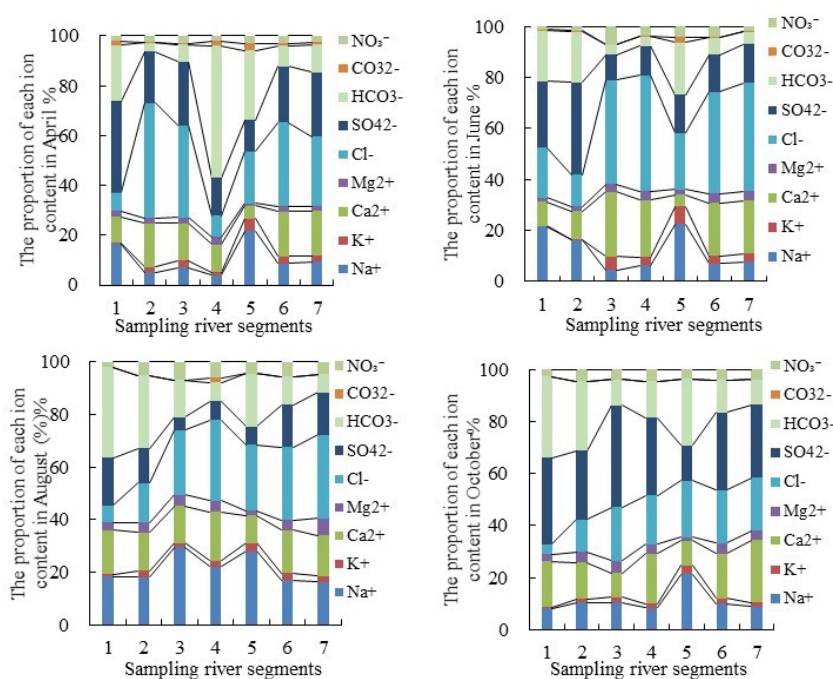


Figure 2. Spatial variation characteristics of main ion contents in surface water in different months (1 Lingdi, 2 Jiaocheng, 3 Dongshihou, 4 Wuliang, 5 Nanxian, 6 Peihui, 7 Sangliushu).

wastewater, industrial enterprises that discharge industrial wastewater, and farms that discharge wastewater, which causes an increase in the number of  $\text{Cl}^-$ ,  $\text{SO}_4^{2-}$ , and  $\text{NO}_3^-$  (Villaverde, 2004) in water in the middle reach. In the lower-reach sampling sites Sangliushu and the Peihui Section, agricultural land dominates and the content of anions saw a certain degree of decline compared to the middle reaches. Among them, for example,  $\text{NO}_3^-$  could be absorbed by plants in water or on river banks as the nitrogen source during its flow (Li *et al.*, 2021a). However, due to the discharge of agricultural wastewater in the lower reaches of the Ciyao River, the concentration of  $\text{NO}_3^-$  is maintained at a high level.

### Hydrochemical types

The Piper diagram can be used to reflect the source of chemical phases of water samples, embody the characteristics of chemical compositions of water bodies, and thus provide the possibility of identifying the general chemical characteristics of water bodies and their control units (Gao and Chen, 2018). By projecting the percentage points of major cations and anions in water bodies to the Piper diagram, the hydrochemical types of various Ciyao River segments are judged.

Based on the Shukarev classification (Gao and Chen 2018, Zhang *et al.*, 2015b) and Piper diagram (Figure 3), the hydrochemical type of the Ciyao River is  $\text{Cl} \cdot \text{SO}_4 \cdot \text{HCO}_3 - \text{Ca} \cdot \text{Na}$ , which indicates that the Ciyao River Basin hydrochemical types could be influenced by the dissolution of carbonates, evaporites, and silicates (Zhang *et al.*, 2015b).

According to Figure 3, it can be observed that the cations in the seven sampling river sections are all close to the  $\text{Ca}^{2+}$  axis, and the distribution of anions is relatively scattered. The cations in the upper ridge bottom section

are dominated by  $\text{Na}^+$  in April and June, and the mixed distribution of  $\text{Na}^+$  and  $\text{Ca}^{2+}$  in August, in October,  $\text{Ca}^{2+}$  dominated. For anions in April, August, and October are dominated by the mixed distribution of  $\text{HCO}_3^-$  and  $\text{SO}_4^{2-}$ . In June, the mixed distribution of  $\text{HCO}_3^-$ ,  $\text{SO}_4^{2-}$  and  $\text{Cl}^-$  is dominant. For Jiaocheng, the cations are dominated by  $\text{Ca}^{2+}$  in April,  $\text{Na}^+$  in June and August, mixed distribution of  $\text{Ca}^{2+}$  and  $\text{Na}^+$  in October,  $\text{Cl}^-$  in April, and  $\text{SO}_4^{2-}$  in June. In April and October, the mixed distribution of  $\text{SO}_4^{2-}$  and  $\text{HCO}_3^-$  dominated. In April and June,  $\text{Ca}^{2+}$  dominated in Dongshihou followed by  $\text{Na}^+$ . In August and October,  $\text{Na}^+$  dominated, followed by  $\text{Ca}^{2+}$ . Anions in April, June, and August are dominated by  $\text{Cl}^-$ , followed by  $\text{SO}_4^{2-}$ , and in October, mainly by  $\text{SO}_4^{2-}$ , followed by  $\text{Cl}^-$ . In August,  $\text{Na}^+$  is dominant, followed by  $\text{Ca}^{2+}$ ; the anions are dominated by  $\text{HCO}_3^-$  in April,  $\text{Cl}^-$  in June and August, while  $\text{SO}_4^{2-}$  in October. In April, June and October,  $\text{Na}^+$  dominated, and the anions are dominated by the mixed distribution of  $\text{HCO}_3^-$ ,  $\text{SO}_4^{2-}$ , and  $\text{Cl}^-$ . The cations in Peihui section are dominated by  $\text{Ca}^{2+}$  in April, June, and October followed by  $\text{Na}^+$ .  $\text{Na}^+$  is dominant in August, followed by  $\text{Ca}^{2+}$ . Anions in April, June, and August were dominated by  $\text{Cl}^-$ , and in October were dominated by the mixed distribution of  $\text{SO}_4^{2-}$  and  $\text{Cl}^-$ . The cations in April, June, and October were dominated by  $\text{Ca}^{2+}$ , and the mixed distribution of  $\text{Na}^+$  and  $\text{Ca}^{2+}$  was dominant in August. The anions in April, June, and August were dominated by  $\text{Cl}^-$ , followed by  $\text{SO}_4^{2-}$ . In October, the mixed distribution of  $\text{SO}_4^{2-}$  and  $\text{Cl}^-$  is the main one.

### Correlation analysis

To further reveal the process and relationship of hydrochemical action of surface water in the Ciyao River (Zhang *et al.*, 2020), we used SPSS software to conduct correlation analyses of hydrochemical metrics. TDS in the

**Table 2.** Correlation analysis of water chemical ions.

Factor	$\text{Na}^+$	$\text{K}^+$	$\text{Ca}^{2+}$	$\text{Mg}^{2+}$	$\text{Cl}^-$	$\text{SO}_4^{2-}$	$\text{HCO}_3^-$	$\text{CO}_3^{2-}$	$\text{NO}_3^-$	TDS
$\text{Na}^+$	1	0.29	0.18	0.26	0.26	0.03	0.511*	0.26	0.35	0.35
$\text{K}^+$		1	0.892**	0.773**	0.854**	0.428*	0.09	0.18	0.925**	0.889**
$\text{Ca}^{2+}$			1	0.885**	0.939**	0.611**	-0.13	0.01	0.893**	0.958**
$\text{Mg}^{2+}$				1	0.828**	0.596*	-0.25	-0.09	0.852**	0.883**
$\text{Cl}^-$					1	0.680**	-0.09	0.14	0.780**	0.974**
$\text{SO}_4^{2-}$						1	-0.03	0.03	0.385*	0.638**
$\text{HCO}_3^-$							1	0.19	0.03	-0.090
$\text{CO}_3^{2-}$								1	0.01	0.121
$\text{NO}_3^-$									1.00	0.865**
Total salt content										1

Note: \*Means correlation is significant at the 0.05 level (both sides). \*\*Means correlation is significant at the 0.01 level (both sides). TDS, total dissolved solids; TH, total hardness.

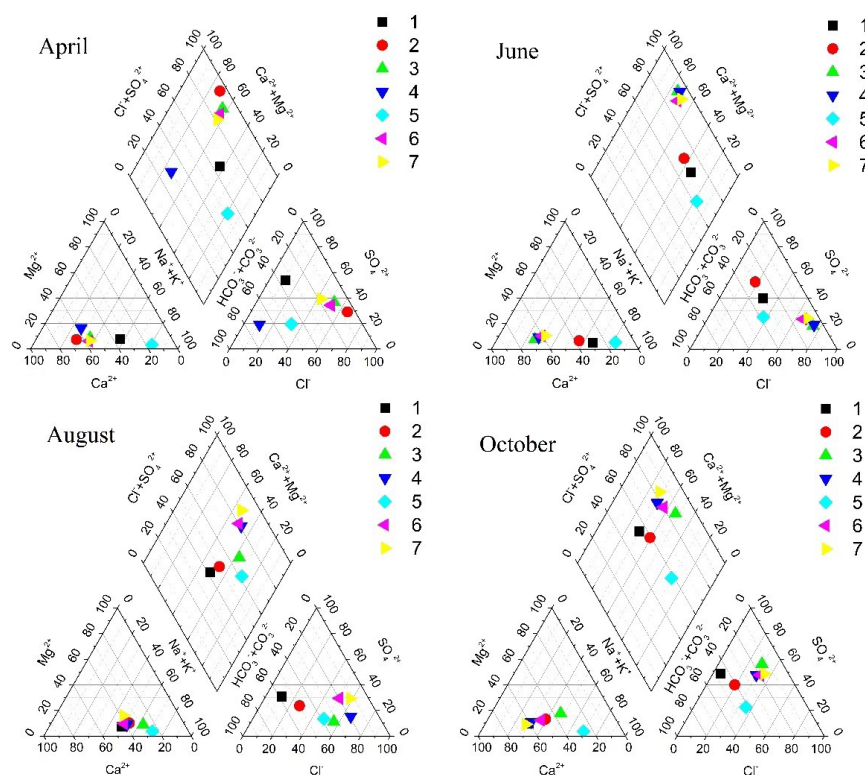


Figure 3. Piper diagram of major ions in surface water (1 Lingdi, 2 Jiaocheng, 3 Dongshihou, 4 Wuliang, 5 Nanxian, 6 Peihui, 7 Sangliushu).

Ciyao River surface water samples was highly correlated with  $K^+$ ,  $Ca^{2+}$ ,  $Mg^{2+}$ , and  $SO_4^{2-}$ , as shown in Table 2. These ions are the main contributors to TDS in surface water.  $K^+$ ,  $Ca^{2+}$ ,  $Mg^{2+}$ ,  $Cl^-$ , and  $SO_4^{2-}$  ions also strongly correlate. These associated ions could be from the same source.

TDS was correlated with most of the major ions to a certain extent, which means that readily soluble components are the main factors that determine TDS. TDS was highly associated with  $Cl^-$ , which means that  $Cl^-$  mainly controls TDS. This shows that the streamflow of this river is mainly from water discharges from urban sewage treatment plants.

### Analysis of hydrochemical genesis

#### Action of cation exchange

The action of alternate adsorption of cations is that under certain conditions, particles will absorb some cations in water and convert some cations previously absorbed into components in water (Hu *et al.*, 2011).  $(Na^+ - Cl^-)$  and  $[2SO_4^{2-} + HCO_3^- - (2Ca^{2+} + 2Mg^{2+})]$  (mmol/L) allow for the decision as to whether the action of  $(Na^+ - Cl^-)$  occurs. If the process of cation exchange mainly dominates hydrogeochemical processes, the ratio of  $(Na^+ - Cl^-)$  to  $[2SO_4^{2-} + HCO_3^- - (2Ca^{2+} + 2Mg^{2+})]$  should be distributed near the 1:1 line.

Based on the relationship diagram of  $(Na^+ - Cl^-)$  and  $[2SO_4^{2-} + HCO_3^- - (2Ca^{2+} + 2Mg^{2+})]$  (Figure 4), it can be seen that the ratios of  $(Na^+ - Cl^-)$  to  $[2SO_4^{2-} + HCO_3^- - (2Ca^{2+} + 2Mg^{2+})]$  in five sites in April were close to each other, the ratios for various river segments in January and June were near the 1:1 line, and the action of cation exchange occurred in April and June, which indicates that in the movement process of river water,  $Ca^{2+}$  and  $Mg^{2+}$  in water was displaced by  $Na^+$  in the outside environment, and the ratios of  $(Na^+ - Cl^-)$  to  $[2SO_4^{2-} + HCO_3^- - (2Ca^{2+} + 2Mg^{2+})]$  in the rest of the months were all far away from the 1:1 line and the action in the hydrogeochemical process was relatively weak.

#### Analysis of sources and controlling factors of major ions

By analyzing hydrochemical components in surface water bodies, the sources of natural hydrochemical compositions are mainly classified into three kinds: vaporization-concentration, rock weathering, and precipitation control. Many scholars used the Gibbs diagram in research on groundwater's chemical components and surface water's chemical compositions (Liu and Liu, 2022; Marandi and Shand, 2018).

To study the natural factors that affect the origin of ions, the relevant importance of various origin mechanisms for ions in river water (effects of atmospheric precipitation, weathering, and evaporation-crystallization) is

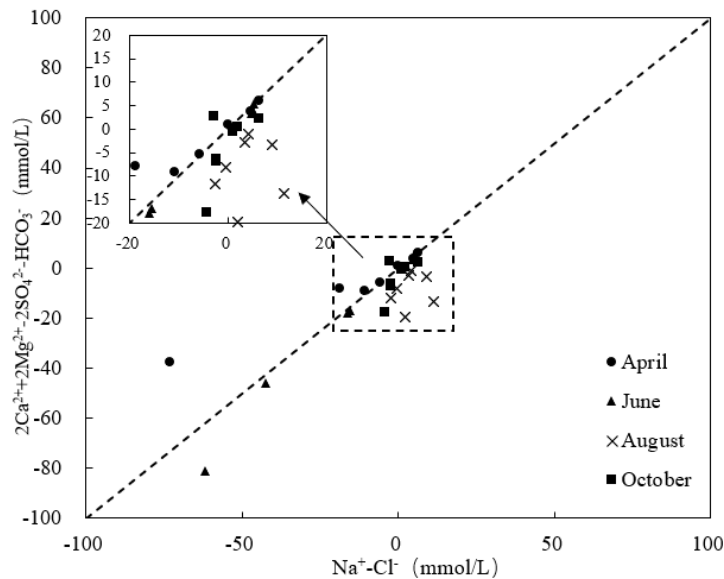


Figure 4. The relationship between  $(\text{Na}^+ - \text{Cl}^-)$  and  $[\text{2SO}_4^{2-} + \text{HCO}_3^- - (\text{2Ca}^{2+} + \text{2Mg}^{2+})]$ .

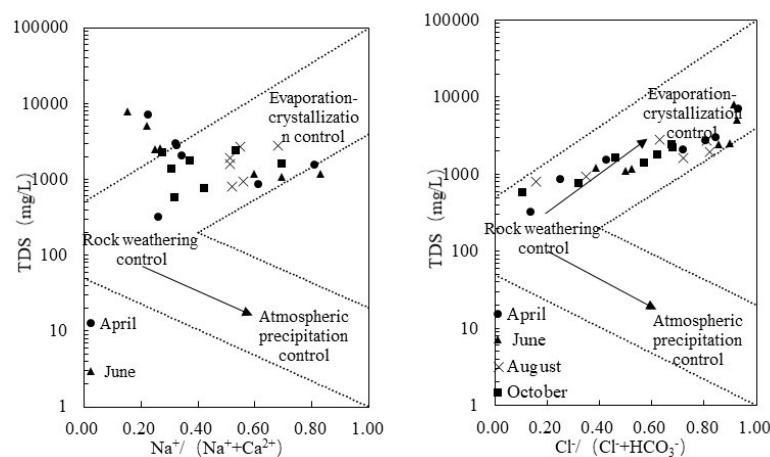


Figure 5. Gibbs diagram of water chemical ions in each reach of Ciyao River.

usually reflected in a macroscopic way using the relationship diagram of the cation's mass concentration  $\text{Na}^+ / (\text{Na}^+ + \text{Ca}^{2+})$  and TDS or the relationship diagram of  $\text{Cl}^- / (\text{Cl}^- + \text{HCO}_3^-)$  and TDS designed by Gibbs. In the control area of action of atmospheric precipitation, the TDS concentration is low ( $\text{TDS} < 10 \text{ mg/L}$ ), and the ratio of  $\text{Na}^+ / (\text{Na}^+ + \text{Ca}^{2+})$  to  $\text{Cl}^- / (\text{Cl}^- + \text{HCO}_3^-)$  is high, normally at 0.5–1. This area is distributed on the lower-right corner of the Gibbs diagram; the action area of rock weathering is located in the middle-left part, with the TDS value normally at 70–300 mg/L and the ratio of  $\text{Na}^+ / (\text{Na}^+ + \text{Ca}^{2+})$  to  $\text{Cl}^- / (\text{Cl}^- + \text{HCO}_3^-)$  normally less than 0.5; the control area of evaporation–crystallization is on the upper-right corner of the diagram, with a higher TDS ( $> 300 \text{ mg/L}$ ) and higher ratios of  $\text{Na}^+ / (\text{Na}^+ + \text{Ca}^{2+})$  and  $\text{Cl}^- / (\text{Cl}^- + \text{HCO}_3^-)$  ( $0.5 = 1$ ).

By calculating the ratios of  $\text{Na}^+ / (\text{Na}^+ + \text{Ca}^{2+})$  and  $\text{Cl}^- / (\text{Cl}^- + \text{HCO}_3^-)$  hydrochemical ions in various segments of the Ciyao River, it was found that the scope of change in both is large, with  $\text{Na}^+ / (\text{Na}^+ + \text{Ca}^{2+})$  between 0.15 and 0.81 and a mean value of 0.45 and  $\text{Cl}^- / (\text{Cl}^- + \text{HCO}_3^-)$  between 0.11 and 0.93, with a mean value of 0.59. From the Gibbs diagram of hydrochemical ions in various segments of the Ciyao River (Figure 5), we can see the relationship between the cation's mass concentration and TDS of the Ciyao River and that except three sections in April and five sections in June, most of the water samples fall into the Gibbs distribution model. The relationship diagrams of the anion's mass concentration and TDS of all sites all fall into the Gibbs distribution model, which means anions in the surface water in the Ciyao River were mainly affected by evaporation–crystallization and

rock weathering, and the difference in different sampling sites is significant. For the Jiaocheng, Dongshihou and Peihui section in April; Dongshihou; Wuliang, the mouth through which the Nanxian, Peihui; and the section of the Sangliushu in June, the relationship sites of the cation's mass concentration and TDS fall outside the range of the Gibbs distribution model, and in seven out of eight out-of-range sampling sites, cation concentrations are all smaller than 0.5, which indicate a great influence of human activities. The sampling sites falling within the model range are Wuliang, Peihui, and the mouth section through which the Fenhe River joins the areas with low mass concentrations of cations. However, the TDS values for these areas are all greater than 300 mg/L, which means that the action of evaporation mainly controlled cations' crystallization (Jang *et al.*, 2017) and is influenced by the control imposed via rock weathering to some extent. With the passage of time, the difference in influences from human activities was big, and an enormous amount of industrial wastewater and urban and rural domestic wastewater was discharged into the river from the lower reach of the Jiaocheng of the Sangliushu is joined, causing changes in the contents of ions in surface water.

The lithological end-element diagram can further indicate differences in rock weathering, including three kinds of weathering of carbonate, silicate, and evaporite rocks, as well as the size of the contribution of the three actions to the source of major ions in water bodies. Weathering of different rocks could result in different ions.  $\text{Ca}^{2+}$  and  $\text{Mg}^{2+}$  mainly resulted from weathering of carbonate, silicate, and evaporite rocks;  $\text{Na}^+$  and  $\text{K}^+$  mainly resulted from weathering and dissolution of silicate and evaporite rocks;  $\text{HCO}_3^-$  mainly resulted from weathering and dissolution of carbonate and silicate rocks; and  $\text{SO}_4^{2-}$  and  $\text{Cl}^-$  mainly resulted from the dissolution of evaporite rocks (Gibbs, 1970). From Figure 6, it can be seen that the sample points of water bodies in the Ciyao River are

mostly distributed between the three end elements of silicate, carbonate, and evaporite rocks, but are distributed more between carbonate and evaporite rocks, which means that the three kinds of rock weathering are the important substance source of the river and the order by the size of the contribution from big to small is carbonate, silicate, and evaporite rocks.

From the relationship diagram of  $\text{Mg}^{2+} + \text{Ca}^{2+}/\text{SO}_4^{2-} + \text{HCO}_3^-$  (Figure 7), it can be seen that most sampling points fall below the  $\text{Mg}^{2+} + \text{Ca}^{2+}/\text{SO}_4^{2-} + \text{HCO}_3^- = 1$  line.  $\text{Ca}^{2+}$  and  $\text{Mg}^{2+}$  are not enough to balance  $\text{SO}_4^{2-}$  and  $\text{HCO}_3^-$ , and  $\text{Na}^+$  and  $\text{K}^+$  are also needed to balance the anions, which means weathering of minerals in carbonate rocks is an important factor that controls hydrochemical content in this area (Li *et al.*, 2021b; Liu *et al.*, 2019b).

From the relationship diagram of  $\text{Cl}^-/\text{Na}^+ + \text{K}^+$  (Figure 7), it can be seen that most of the sampling sites fall below the 1:1 line, which means  $\text{Na}^+$  and  $\text{K}^+$  are not enough to balance  $\text{Cl}^-$ , and other cations are also needed to balance  $\text{Cl}^-$ ; the excess portion of  $\text{Cl}^-$  mainly resulted from the dissolution of evaporite rocks.

## Conclusion

1. Surface water in the Ciyao River was weakly alkaline. The contents of TDS were greatly and spatially different and holistically exhibited a trend of middle reach > lower reach > upper reach in the basin.
2. The study basin is a freshwater area with  $\text{Na}^+$  and  $\text{Ca}^{2+}$  as the main cations and  $\text{Cl}^-$  and  $\text{SO}_4^{2-}$  as the main anions, and the hydrochemical types are  $\text{Cl} \cdot \text{SO}_4 \cdot \text{HCO}_3 - \text{Ca} \cdot \text{Na}$ .
3. The hydrochemical compositions of the Ciyao River were controlled by rock weathering, evaporation–crystallization, and human activities, and influenced by the action of cation exchange to some extent. The

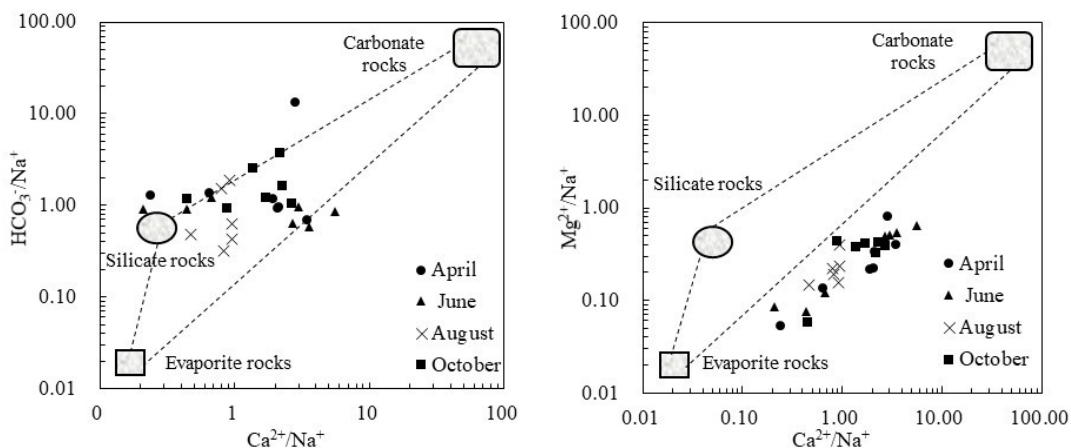


Figure 6. Relationship between  $\text{Ca}^{2+}/\text{Na}^+$  and  $\text{Mg}^{2+}/\text{Na}^+$  and  $\text{Ca}^{2+}/\text{Na}^+$  and  $\text{HCO}_3^-/\text{Na}^+$ .

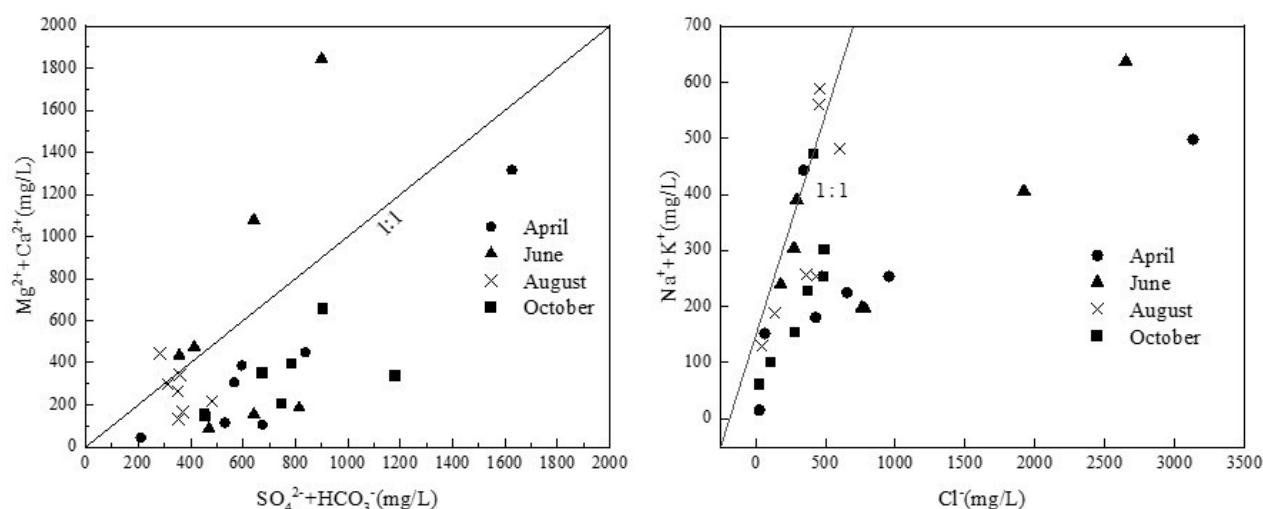


Figure 7. Relationship between  $\text{SO}_4^{2-} + \text{HCO}_3^-$  and  $\text{Mg}^{2+} + \text{Ca}^{2+}$  and  $\text{Cl}^-$  and  $\text{Na}^+ + \text{K}^+$ .

order by the extent of influence of rock weathering on the composition of ions in this basin from large to small is carbonate, silicate, and evaporate rocks. Meanwhile, evaporation–crystallization, construction land–dominated land-use types, and industrial and domestic wastewater discharge also greatly impacted the hydrochemical compositions. Therefore, programs to reduce the emission of pollution sources in the vicinity of the Ciyao River are recommended.

## Competing Interests

The authors declare that they have no conflict of interest to report.

## Availability of Data

Please contact the author for data requests.

## Funding

The Key R&D Program of Shanxi Province (201903D311004); Applied Basic Research Program of Shanxi Province (201801D221335); Top Young Talent Support Program of Shanxi Province

## References

Bai, B., Bai, F., Li, X., Nie, Q., Jia, X. and Wu, H., 2022. The remediation efficiency of heavy metal pollutants in water by industrial red mud particle waste. *Environmental Technology & Innovation* 25: 102944. <https://doi.org/10.1016/j.eti.2022.102944>

- Chen, X., Quan, Q., Zhang, K. and Wei, J., 2021. Spatiotemporal characteristics and attribution of dry/wet conditions in the Weihe River Basin within a typical monsoon transition zone of East Asia over the recent 547 years. *Environmental Modelling & Software* 143: 105116. <https://doi.org/10.1016/j.envsoft.2021.105116>
- Dai, L., Wang, Z., Guo, T., Hu, L., Chen, Y., Chen, C., Yu, G., Ma, L.Q. and Chen, J., 2022. Pollution characteristics and source analysis of microplastics in the Qiantang River in southeastern China. *Chemosphere* 293: 133576. <https://doi.org/10.1016/j.chemosphere.2022.133576>
- Devivo, B., Belkin, H. and Lima, A., 2017. *Environmental geochemistry: site characterization, data analysis and case histories*, Elsevier Science, Amsterdam.
- Fang, X., Wang, Q., Wang, J., Xiang, Y., Wu, Y. and Zhang, Y., 2021. Employing extreme value theory to establish nutrient criteria in bay waters: a case study of Xiangshan Bay. *Journal of Hydrology* 603: 127146. <https://doi.org/10.1016/j.jhydrol.2021.127146>
- Fu, G., Butler, D. and Khu, S.-T., 2009. The impact of new developments on river water quality from an integrated system modelling perspective. *Science of the Total Environment* 407: 1257–1267. <https://doi.org/10.1016/j.scitotenv.2008.10.033>
- Gao, Z. and Chen, C., 2018. The classification method of water chemical types based on the principle of Kurllov's formula and Shoka Lev classification. *Groundwater* 40: 6–13.
- Ge, D., Yuan, H., Xiao, J. and Zhu, N., 2019. Insight into the enhanced sludge dewaterability by tannic acid conditioning and pH regulation. *Science of The Total Environment* 679: 298–306. <https://doi.org/10.1016/j.scitotenv.2019.05.060>
- Gibbs, R.J., 1970. Mechanisms controlling world water chemistry. *Science* 170: 1088–1090. <https://doi.org/10.1126/science.170.3962.1088>
- Hu, C., Zhou, W. and Xia, S., 2011. Characteristics of major ions and the influence factors in Poyang Lake catchment. *Environmental Chemistry* 30: 1620–1626.
- Huiwei, W., Xiaojiao, G., Zhang, Q. and Bingyan, L., 2021. Evolution of groundwater hydrochemical characteristics and origin analysis in Hutuo River Basin. *Environmental Chemistry* 40: 3838–3845.

- Jang, E., Jeong, S. and Chung, E., 2017. Application of three different water treatment technologies to shale gas produced water. *Geosystem Engineering* 20: 104–110. <https://doi.org/10.1080/12269328.2016.1239553>
- Jia, Y., Guo, H., Xi, B., Jiang, Y., Zhang, Z., Yuan, R., Yi, W. and Xue, X., 2017. Sources of groundwater salinity and potential impact on arsenic mobility in the western Hetao Basin, Inner Mongolia. *Science of the Total Environment* 601: 691–702. <https://doi.org/10.1016/j.scitotenv.2017.05.196>
- Ke, Z., Bai, Y., Bai, Y., Chu, Y., Gu, S., Xiang, X., Ding, Y. and Zhou, X., 2022. Cold plasma treated air improves the characteristic flavor of dry-cured black carp through facilitating lipid oxidation. *Food Chemistry* 377: 131932. <https://doi.org/10.1016/j.foodchem.2021.131932>
- Li, J., Jiang, Y. and Liu, Y., 2022. Hydrogeochemical characteristics and spatial-temporal variations of groundwater in the Liangshui River basin, Beijing. *Chinese Environmental Science* 42: 7–12.
- Li, L.-J., Li, H.-B. and Wang, J., 2002. Analysis on hydrological and water quality character and their spatial and temporal distribution in Lancangjiang River. *Scientia Geographica Sinica/Dili Kexue* 22: 49–56.
- Li, M., Jiang, T., He, R., Mu, Z., Wei, S. and Xie, D., 2012. Water chemistry characteristics of a typical agricultural small watershed in Three Gorge Reservoir area and its changing tendency. *China Environmental Science* 32: 1062–1068.
- Li, S., Cui, G. and Li, Q., 2018. Hydrochemical characteristics and spatial-temporal distribution of nitrogen and silicon in cascade reservoirs of the Jialing River. *Earth and Environment* 46: 10–16.
- Li, W., Shi, Y., Zhu, D., Wang, W., Liu, H., Li, J., Shi, N., Ma, L. and Fu, S., 2021a. Fine root biomass and morphology in a temperate forest are influenced more by the nitrogen treatment approach than the rate. *Ecological Indicators* 130: 108031. <https://doi.org/10.1016/j.ecolind.2021.108031>
- Li, Y.-Z., Gao, Z.-J., Liu, J.-T., Wang, M. and Han, C., 2021b. Hydrogeochemical and isotopic characteristics of spring water in the Yarlung Zangbo River Basin, Qinghai-Tibet Plateau, Southwest China. *Journal of Mountain Science* 18: 2061–2078. <https://doi.org/10.1007/s11629-020-6625-y>
- Lin, X., Lu, K., Hardison, A.K., Liu, Z., Xu, X., Gao, D., Gong, J. and Gardner, W.S., 2021. Membrane inlet mass spectrometry method (REOX/MIMS) to measure  $^{15}\text{N}$ -nitrate in isotope-enrichment experiments. *Ecological Indicators* 126: 107639. <https://doi.org/10.1016/j.ecolind.2021.107639>
- Liu, F., Wang, S., Wang, L., Shi, L., Song, X., Yeh, T.-C.J. and Zhen, P., 2019a. Coupling hydrochemistry and stable isotopes to identify the major factors affecting groundwater geochemical evolution in the Heilongdong Spring Basin, North China. *Journal of geochemical Exploration* 205: 106352. <https://doi.org/10.1016/j.gexplo.2019.106352>
- Liu, J., Gao, Z., Wang, M., Li, Y., Shi, M., Zhang, H. and Ma, Y., 2019b. Hydrochemical characteristics and possible controls in the groundwater of the Yarlung Zangbo River Valley, China. *Environmental Earth Sciences* 78: 1–11. <https://doi.org/10.1007/s12665-019-8101-y>
- Liu, J. and Liu, J., 2022. Hydrochemical characteristics analysis and hydrogeochemical simulation of shallow groundwater in downstream of Haihe River Basin. *Energy and Environmental Protection* 2022: 6–13.
- Liu, J.-T., Cai, W.-T., Cao, Y.-T., Cai, Y.-M., Bian, C., Lü, Y.-G. and Chen, Y.-M., 2018. Hydrochemical characteristics of groundwater and the origin in alluvial-proluvial fan of Qinhe River. *Huan Jing ke Xue = Huanjing Kexue* 39: 5428–5439.
- Liu, M., Zhao, L. and Li, Q., 2021a. Hydrochemical characteristics, main ion sources of main rivers in the source region of Yangtze River. *China Environmental Science* 41: 1243–1254.
- Liu, X., Xiang, W. and Ma, X., 2021b. Hydrochemical characteristics and controlling factors of shallow groundwater in the Chinese Loess Plateau. *Chinese Environmental Science* 41: 9–14.
- Liu, Y., Tian, J., Zheng, W. and Yin, L., 2022. Spatial and temporal distribution characteristics of haze and pollution particles in China based on spatial statistics. *Urban Climate* 41: 101031. <https://doi.org/10.1016/j.uclim.2021.101031>
- Liu, Y., Zhang, K., Li, Z., Liu, Z., Wang, J. and Huang, P., 2020. A hybrid runoff generation modelling framework based on spatial combination of three runoff generation schemes for semi-humid and semi-arid watersheds. *Journal of Hydrology* 590: 125440. <https://doi.org/10.1016/j.jhydrol.2020.125440>
- Luo, Z., Renzeng, L. and Chen, H., 2021. Hydrochemical characteristics and its controlling factors of Basong Lake in cold season in Tibet. *Chinese Environmental Science* 41: 8–13.
- Marandi, A. and Shand, P., 2018. Groundwater chemistry and the Gibbs Diagram. *Applied Geochemistry* 97: 209–212. <https://doi.org/10.1016/j.apgeochem.2018.07.009>
- Markich, S.J. and Brown, P.L., 1998. Relative importance of natural and anthropogenic influences on the fresh surface water chemistry of the Hawkesbury–Nepean River, south-eastern Australia. *Science of the Total Environment* 217: 201–230. [https://doi.org/10.1016/S0048-9697\(98\)00188-0](https://doi.org/10.1016/S0048-9697(98)00188-0)
- Ning, T., Li, Z. and Liu, W., 2016. Separating the impacts of climate change and land surface alteration on runoff reduction in the Jing River catchment of China. *Catena* 147: 80–86. <https://doi.org/10.1016/j.catena.2016.06.041>
- Pant, R.R., Zhang, F., Rehman, F.U., Wang, G., Ye, M., Zeng, C. and Tang, H., 2018. Spatiotemporal variations of hydrogeochemistry and its controlling factors in the Gandaki River Basin, Central Himalaya Nepal. *Science of the Total Environment* 622: 770–782. <https://doi.org/10.1016/j.scitotenv.2017.12.063>
- Peng, X., Zheng, J., Liu, Q., Hu, Q., Sun, X., Li, J., Liu, W. and Lin, Z., 2021. Efficient removal of iron from red gypsum via synergistic regulation of gypsum phase transformation and iron speciation. *Science of The Total Environment* 791: 148319. <https://doi.org/10.1016/j.scitotenv.2021.148319>
- Qi, X., Liu, S. and Zhang, Z., 2021. Emporal and spatial variation and cause analysis of shallow groundwater chemistry in Binzhou City. *Earth and Environment* 19: 1–11.
- Quan, Q., Gao, S., Shang, Y. and Wang, B., 2021. Assessment of the sustainability of *Gymnocypis eckloni* habitat under river damming in the source region of the Yellow River. *Science of the Total Environment* 778: 146312. <https://doi.org/10.1016/j.scitotenv.2021.146312>
- Ruxue, L., 2021. Assessment of self-purification capacity of tailwater recharge-type rivers in urban sewage plants and its influencing

- factors. *Environmental Science and Pollution Research* 21: 10583–10593.
- Shen, Z., 1983. Hydrogeochemical basis. *Hydrogeology Engineering Geology* 3: 58–61.
- Tian, H., Qin, Y., Niu, Z., Wang, L. and Ge, S., 2021. Summer maize mapping by compositing time series sentinel-1A imagery based on crop growth cycles. *Journal of the Indian Society of Remote Sensing* 49: 2863–2874. <https://doi.org/10.1007/s12524-021-01428-0>
- Villaverde, S., 2004. Recent developments on biological nutrient removal processes for wastewater treatment. *Re/Views in Environmental Science & Bio/Technology* 3: 171–183. <https://doi.org/10.1007/s11157-004-4565-6>
- Williams, M.R., Fisher, T.R. and Melack, J.M., 1997. Solute dynamics in soil water and groundwater in a central Amazon catchment undergoing deforestation. *Biogeochemistry* 38: 303–335. <https://doi.org/10.1023/A:1005801303639>
- Wu, C., Xuan, Y. and Zhang, H., 2015. Groundwater hydrochemical characteristics and cause analysis in an arid and semi-arid area South-to-North Water Diversion. *Water Conservancy Technology* 5: 1–15.
- Wu, X., Liu, Z., Yin, L., Zheng, W., Song, L., Tian, J., Yang, B. and Liu, S., 2021. A haze prediction model in chengdu based on LSTM. *Atmosphere* 12: 1479. <https://doi.org/10.3390/atmos12111479>
- Xu, J., Lan, W., Ren, C., Zhou, X., Wang, S. and Yuan, J., 2021. Modeling of coupled transfer of water, heat and solute in saline loess considering sodium sulfate crystallization. *Cold Regions Science and Technology* 189: 103335. <https://doi.org/10.1016/j.coldregions.2021.103335>
- Yan, Y., Niu, F. and Liu, J., 2022. Hydrochemical characteristics and sources of the upper Yarlung Zangbo River in summer *Chinese Environmental Science* 42: 11–15.
- Yang, Y., Li, T., Wang, Y., Cheng, H., Chang, S.X., Liang, C. and An, S., 2021. Negative effects of multiple global change factors on soil microbial diversity. *Soil Biology and Biochemistry* 156: 108229. <https://doi.org/10.1016/j.soilbio.2021.108229>
- Yin, L., Wang, L., Huang, W., Liu, S., Yang, B. and Zheng, W., 2021. Spatiotemporal analysis of haze in Beijing based on the multi-convolution model. *Atmosphere* 12: 1408. <https://doi.org/10.3390/atmos12111408>
- Yin, L., Wang, L., Zheng, W., Ge, L., Tian, J., Liu, Y., Yang, B. and Liu, S., 2022. Evaluation of empirical atmospheric models using Swarm-C satellite data. *Atmosphere* 13: 294.
- Zhang, K., Wang, S., Bao, H. and Zhao, X., 2019. Characteristics and influencing factors of rainfall-induced landslide and debris flow hazards in Shaanxi Province, China. *Natural Hazards and Earth System Sciences* 19: 93–105. <https://doi.org/10.5194/nhess-19-93-2019>
- Zhang, Q., Jin, Z., Zhang, F. and Xiao, J., 2015a. Seasonal variation in river water chemistry of the middle reaches of the Yellow River and its controlling factors. *Journal of Geochemical Exploration* 156: 101–113. <https://doi.org/10.1016/j.gexplo.2015.05.008>
- Zhang, T., Wang, M.-G., Zhang, Z.-Y., Liu, T. and He, J., 2020. Hydrochemical characteristics and possible controls of the surface water in ranwu lake basin. *Huan Jing ke Xue = Huanjing Kexue* 41: 4003–4010.
- Zhang, X., Ma, F., Dai, Z., Wang, J., Chen, L., Ling, H. and Soltanian, M.R., 2022. Radionuclide transport in multi-scale fractured rocks: a review. *Journal of Hazardous Materials* 424: 127550. <https://doi.org/10.1016/j.jhazmat.2021.127550>
- Zhang, X., Ma, F., Yin, S., Wallace, C.D., Soltanian, M.R., Dai, Z., Ritzi, R.W., Ma, Z., Zhan, C. and Lü, X., 2021. Application of upscaling methods for fluid flow and mass transport in multi-scale heterogeneous media: a critical review. *Applied Energy* 303: 117603.
- Zhang, Y., Wu, Y., Yang, J. and Sun, H., 2015b. Hydrochemical characteristic and reasoning analysis in Siyi Town, Langzhong City. *Huan Jing ke Xue = Huanjing Kexue* 36: 3230–3237.
- Zhao, T., Shi, J., Entekhabi, D., Jackson, T.J., Hu, L., Peng, Z., Yao, P., Li, S. and Kang, C.S., 2021. Retrievals of soil moisture and vegetation optical depth using a multi-channel collaborative algorithm. *Remote Sensing of Environment* 257: 112321. <https://doi.org/10.1016/j.rse.2021.112321>
- Zongxing, L., Qi, F., Wang, Q., Song, Y., Jianguo, L., Yongge, L. and Yamin, W., 2016. Quantitative evaluation on the influence from cryosphere meltwater on runoff in an inland river basin of China. *Global and Planetary Change* 143: 189–195. <https://doi.org/10.1016/j.gloplacha.2016.06.005>